NANO LETTERS

pubs.acs.org/NanoLett

Probing Strain in Bent Semiconductor Nanowires with Raman Spectroscopy

Jianing Chen, Gabriela Conache, Mats-Erik Pistol, Struan M. Gray, Magnus T. Borgström, Hongxing Xu, H. Q. Xu, Lars Samuelson, and Ulf Håkanson*

The Nanometer Structure Consortium/Division of Solid State Physics, Lund University, Sweden

ABSTRACT We present a noninvasive optical method to determine the local strain in individual semiconductor nanowires. InP nanowires were intentionally bent with an atomic force microscope and variations in the optical phonon frequency along the wires were mapped using Raman spectroscopy. Sections of the nanowires with a high curvature showed significantly broadened phonon lines. These observations together with deformation potential theory show that compressive and tensile strain inside the nanowires is the physical origin of the observed phonon energy variations.

KEYWORDS Nanowire, strain mapping, Raman spectroscopy, phonon shift

The unique geometry and properties of semiconductor nanowires (NWs) have stimulated their use for novel devices.[1−3] To optimize their application, a detailed understanding of the NW material properties is of great importance. For example, it has been found that NW crystal structures are affected by and can be controlled with their growth parameters.[4,5] In addition, even though the NW geometry allows for efficient strain relaxation via the surface, strain is in general known to alter the band structure in semiconductors,[6] which has an impact in complex NW geometries.[7] Externally applied forces will also affect the electronic properties of the NWs, and information about the strain distribution within the wires becomes important for applications utilizing deformation of the NWs such as, for example, probing their piezoelectric response.[8]

Elaborate techniques do exist to investigate strain in nanowire systems, ranging from four point probe scanning tunnelling microscopy[9] to transmission electron microscopy (TEM).[10] The latter technique has been shown to be a versatile tool for obtaining structural and chemical information with atomic resolution.[10−14] Unfortunately TEM is experimentally challenging since it is time-consuming and requires high-vacuum conditions. Special care must also be taken during inspection of nanostructures such as nanowires to avoid electron beam-induced damage[15] or carbon deposition[16] that can affect the measured properties of the sample being investigated.

To access chemical information in a simple, fast, and noninvasive manner and with a comparable resolution would therefore open up a new avenue for device characterization. Raman spectroscopy is a candidate for approaching this goal, since it is a well-established technique for characterizing the crystal structure of semiconductors. It further offers detailed information about lattice excitations and is therefore an important complement to spectroscopy in probing the electronic states. Raman spectroscopy has previously been used to study material properties such as crystal structure, composition, mechanical strain, doping, and phonon confinement.[17]

Lately, several groups have used Raman microscopy to characterize nanowire systems, including III−V semiconductors materials such as GaP,[18] InAs,[19] GaAs,[19,20] and GaN[21] as well as II−VI materials such as ZnS[22,23] and ZnO.[24] The main interest has been to investigate NW confinement effects,[22,25−28] surface optical modes,[18,22] and antenna properties[29] caused by the wires' large surface-to-volume ratios. To date, however, there are only a few papers that address the crystal structure of semiconductor NWs in a Raman context; Begum et al. discussed the structural properties of individual nanowires and related the observed downshift of the phonon modes to structural defects within them.[19] They identified, by point spectroscopy along a single wire, crystal quality variations and differences in defect densities between individual wires from the same batch. Lopez et al. showed the benefits of high-throughput Raman analyses by performing correlated Raman microscopy and TEM characterization and thereby identified polytypes, planar defects, and the distribution of stacking faults in individual Si NWs.[14] Pauzauskie et al. investigated single U-shaped NWs and convincingly showed that polarized Raman spectroscopy, in combination with Raman mapping using a scanning stage, is a powerful way to obtain information on crystal structure, growth direction, and radial crystallographic orientation.[21] A resolution on the order of 200 nm is obtained, far below the diffraction limit for the laser wavelength used, making the technique highly suitable for local scale analysis of nanostructures. The authors further propose that this technique could be suitable for observing

* To whom correspondence should be addressed. E-mail: ulf.hakanson@ftf.lth.se.

Received for review: 12/6/2009
Published on Web: 03/01/2010

DOI: 10.1021/nl904040y | *Nano Lett.* **2010,** *10,* 1280–1286

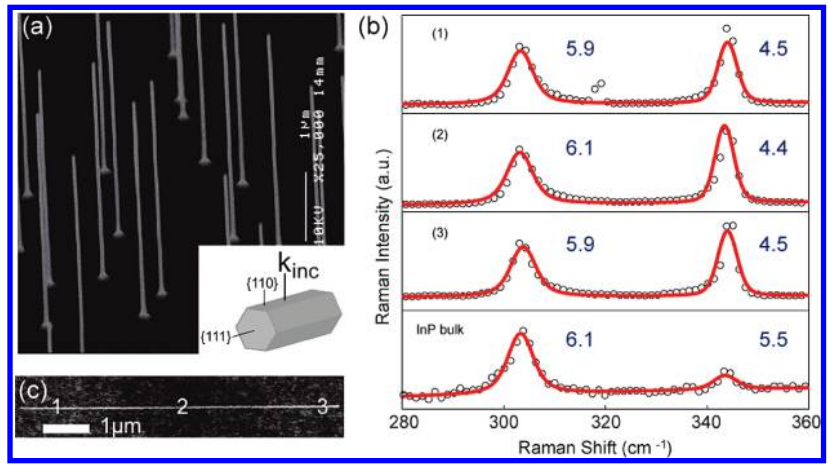

FIGURE 1. (a) SEM image of the 7.5 μm long nanowires as grown (the image was taken at an angle of 30° toward the normal of the (111) plane). The inset depicts the experimental configuration. For details see text. (b) Normalized single point Raman spectra (open circles) acquired along the wire shown in (c). The corresponding focus positions are indicated with numbers in (c). A Raman spectrum from bulk InP is shown for comparison. Red solid lines are least-squares fits of Voigt lineshapes to the experimental data, and corresponding values for the fwhm are indicated in the figure. (c) An SEM image of a single nanowire deposited on an Au substrate.

stress in single NWs. No such effects were, however, observed in their experimental work.

In the present study, we report on the first Raman investigations of strain in bent NWs. Individual InP NWs were manipulated and bent in a controlled fashion by the tip of an atomic force microscope (AFM)[30,31] and studied by Raman spectroscopy. Raman spectra were collected along the bent wires and strain broadened phonon lines were observed in sections of the wire with large curvature. Deformation potential theory together with careful analysis of the NW curvature allows us independently to determine the strain in the wires and quantitatively correlate the broadening of the Raman spectra to the measured strain.

InP nanowires were grown by metal−organic vapor phase epitaxy (see Supporting Information for details of the growth). The grown NWs are frequently twinned[32] and about 7.5 μm in length. The cross section of the nanowires appears hexagonal, but the nanowire side facets are probably a dense mixture of (111)A and (111)B facets due to the high-stacking fault density in the Sn-doped, n-type wurtzite (WZ) nanowires.[32] Scanning electron microscopy (SEM) was used to determine the length of the wires; an example image is shown in Figure 1a.

For optical characterization and AFM imaging and manipulation, the nanowires were mechanically transferred to patterned SiO_2 substrates onto which a 150 nm thick gold film had been thermally evaporated.

Raman measurements were performed with a standard fiber-coupled Raman microscope system (InduRAM, HORIBA Jobin Yvon) equipped with a motorized stage (minimum step 100 nm). Raman signals are obtained in a backscattering configuration using a 100× objective (NA 0.9) and a HeNe laser with a wavelength of 632.8 nm. The laser spot size is about 1 μm, which in combination with the imaging capabilities of the microscope allows for routine single wire identification. A laser power below 0.5 mW was used to avoid heating effects. Further information about our experimental method can be found in the Supporting Information.

Figure 1a shows InP NWs grown on an InP substrate. The wires are homogeneous both in width and height which demonstrates our ability to grow morphologically nearly identical nanowires, critical for high-yield production of nanowire devices. Raman spectra from an individual wire are shown in Figure 1b. For clarity, three spectra are shown from a line scan along the wire. All spectra display two clear phonon modes which can be associated with the transverse-optical mode (TO) at 304 cm^{-1} and the longitudinal-optical (LO) mode at 344 cm^{-1}. The two phonon modes are expected to be present in the Raman spectra for hexagonal NWs measured in a backscattering geometry.[17,20] This assumes that the wire rests with a flat side on the surface, which has been confirmed.[30,31]

To quantify the observed phonon modes, we have made least-squares fits to the obtained Raman spectra. It is common to use a Voigt line shape function when fitting a measured Raman line from a semiconductor material, in which each Raman peak is a convolution of the intrinsic phonon mode, having a Lorentzian line shape, and the instrumental response, having a Gaussian line shape. The presence of inhomogeneous strain in the bent nanowires further complicates the situation, and for these wires we convolve a further Gaussian broadening function to model how the strain influences the Raman bands. This allows us to treat all spectra in a consistent manner. Details of the fitting procedure are given in the Supporting Information.

As shown in Figure 1, the high signal-to-noise in the data allows us clearly to determine the peak position and full-width-at-half-maximum (fwhm) of the Raman spectra. A conservative estimate of the accuracies in the fits is 0.5 cm^{-1}, which is also the nominal resolution of the spectrometer.

For comparison, we performed measurements on bulk InP samples giving highly symmetric Raman peaks centered

DOI: 10.1021/nl904040y | *Nano Lett.* **2010,** *10,* 1280–1286

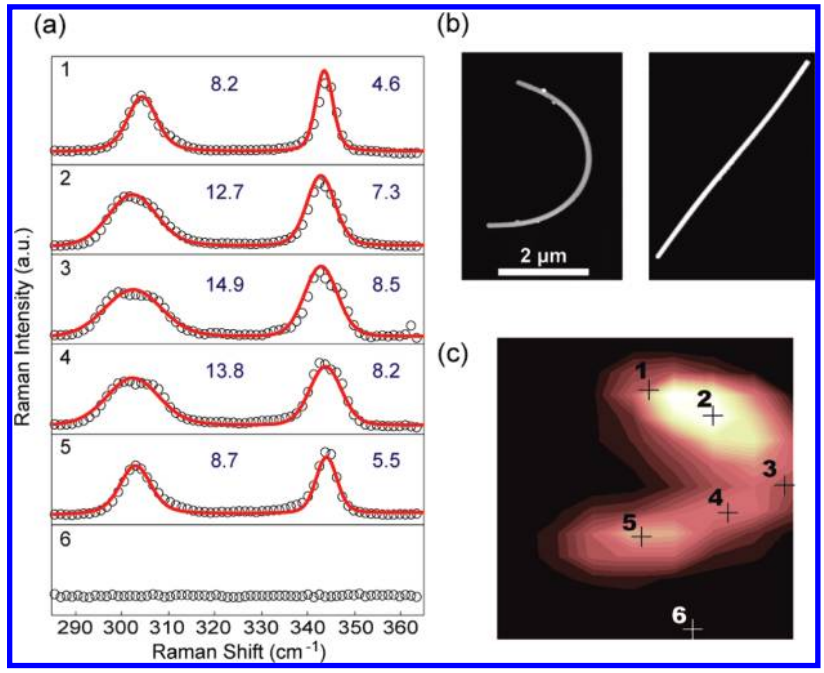

FIGURE 2. Raman investigations of an individual bent nanowire. (a) Normalized Raman spectra acquired at five different positions (1−5) along the bent nanowire shown to the left in (b) together with a reference spectrum (6). Adjacent to the Raman peaks the fwhm of the fitted Voigt profile is given in wavenumbers. (b) AFM image of the bent wire (left) and of the same wire prior to bending (right). (c) Raman image generated by integrating the signal over a frequency band covering the two phonon modes (ca. 290−350 cm^{-1}). Also indicated in the figure are also the central positions of the laser focus corresponding to the spectra in (a).

at 304 and 344 cm^{-1} for the TO, and LO modes respectively (c.f. Figure 1). Our results, both for individual NWs and bulk, agree well with reported bulk values[33] suggesting a high crystal quality for our NW samples. The measured widths of the Raman peaks are also in good agreement.

Line scans along the wires further show that there are only very small variations in the position and line width of the Raman peaks, as is demonstrated in Figure 1b. In total, we measured 20 spectra along this wire with a step size of 200 nm obtaining similar results in all of them. We have investigated more than 20 NWs in this manner, and all exhibit the same behavior. To ensure that single wires were investigated, the sample was characterized by high-resolution SEM. Bundles of thinner NWs were occasionally observed but could easily be excluded from the experiments using SEM or AFM.

Having verified that there are no significant variations in the Raman spectra of the wires as grown, we investigated the effect of strain on their phonon modes. The NWs were bent by pushing on them with an AFM tip. A Nanoscope IIIa Dimension 3100 AFM from Veeco Instruments was used with Si tips having a spring constant in the range 30−40 N/m. The wires were pushed on one end at a time, typically at a distance from the end one-fourth to one-eighth of the length of the nanowire. The manipulation procedure is described in detail in refs 30 and 31.

After manipulation the nanowires are pinned in a curved shape by friction at the interface with the substrate.[30] Obviously, the higher the curvature, the larger the strain within the wire will be. If we assume that the nanowire can be described by the Euler theory of beam-bending with a neutral axis along its center, then for wires whose radius, r, is small compared to the bending radius, $R(z)$, the strain will vary linearly from the inside of the curve to the outside with a maximum value at the edges of $\varepsilon(z) = \pm r/R(z)$. We neglect the shear component across the wire created by the spatially varying value for $\varepsilon(z)$, as well as the more complicated shear field set up because friction with the substrate only takes place on its bottom facet. Experimentally, the curvature of the nanowire is found by tracing its backbone in the AFM image, as described in ref 31.

Figure 2 summarizes a Raman investigation of a bent NW. By recording Raman spectra in steps of 200 nm over a preselected area spectral mapping of the NW can be achieved. From the acquired data we can generate a Raman image by, for example, integrating the signal over a frequency band covering the two phonon modes (ca. 290−350 cm^{-1}). The resulting "optical image" in Figure 2c allows us to extract the Raman spectrum for any given position within the scan range. In Figure 2a, this is exemplified by Raman spectra at five different positions (1−5) along the wire as well as from a reference point (6). In contrast to the straight wires, we observe clear changes in the phonon modes as different parts of the wire are probed. Spectra 2−4 are measured at positions close to the region with highest curvature, and consequently the highest strain. All three spectra are clearly broadened compared to straight wires. At position 3 the TO mode is almost 3 times as broad whereas the LO mode is

DOI: 10.1021/nl904040y | *Nano Lett.* **2010,** *10,* 1280–1286

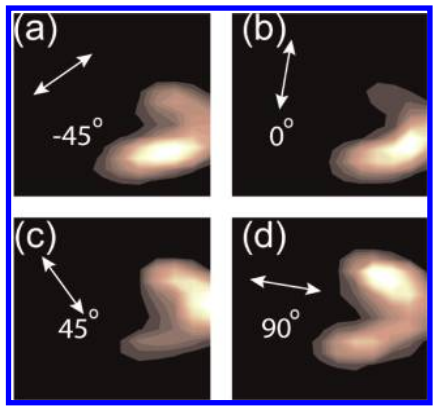

FIGURE 3. Polarization investigation of an individual bent nanowire. (a−d) Raman images generated by integrating the signal over a frequency band covering the two phonon modes (ca. 290−350 cm^{-1}). The white arrows show the polarization direction of the incident light used.

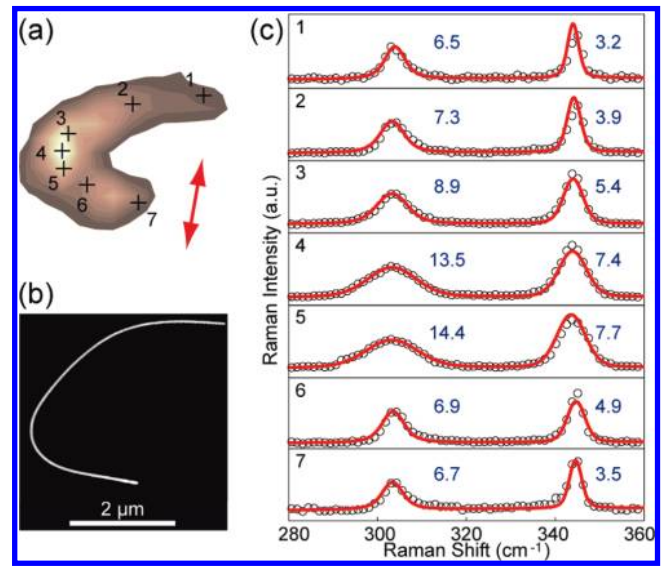

FIGURE 4. (a) Raman image generated by integrating the signal over a frequency band covering the two phonon modes (ca. 290−350 cm^{-1}). Also indicated in the figure are the central positions of the laser focus corresponding to the Raman spectra in (c) The red arrow shows the polarization of the incident light. (b) An AFM image of the bent nanowire. The diameter of the wire was determined to be 44 nm. (c) Raman spectra acquired at different positions (1−7) along the nanowire shown in (b).

roughly doubled. Qualitatively, the broadening of the phonon modes can be explained by the fact that the NWs experience compressive strain on the inner side of the curve and tensile strain on the outer side,[13] both of which are probed by the laser spot. Compression leads to a positive frequency shift of the phonon modes, whereas tension induces a negative shift;together, the two produce a broadening.

Before comparing our experimental findings quantitatively with theoretical calculations, we address the polarization dependence of one-dimensional structures. Small diameter nanowires can be considered to act as ideal dipole antennas, leading to a polarization dependence which follows a simple $\cos^2(\phi)$ function, where ϕ is the angle between the NW axis and the incident electric field. The large shape anisotropy, combined with the high dielectric contrast between the wire and the surrounding media,[34] leads to a strong scattering signal only for light polarized parallel to the NW axis.[22,29,35]

For the bent wires, the intensity distribution is more complex. In Figure 3, we show four Raman maps acquired under the same experimental conditions, except we have varied the polarization of the incident light. As the polarization plane of the incoming light is rotated the intensity distribution of the scattered light from the NW is altered. Although the scattering signal intensity varies in different regions of the nanowire when the polarization is changed, we do not observe any spectral changes that depend on the polarization direction. Example spectra are shown in the Supporting Information.

The selection rules are complicated for nanowire systems, having many crystal facets as well as stacking faults. The situation is even more complicated for bent nanowires, making it hard to predict how the system responds to different polarization configurations. We have tried to identify spatial variations along the wires for the LO and TO bands separately, but no differences could be observed.

Interestingly, the phonon modes appear to be slightly modified even at positions 1 and 5, which are measured at positions far from the region with highest strain (cf. Figure 2). One should however remember that regions close to the wire ends are still slightly bent with a strain of about 0.5%, as is shown later in Figure 5. In addition, the strong polarization dependence of the Raman intensity described above in combination with possible wave guiding phenomena often observed in nanowire systems[36] makes it difficult to determine the exact extent of the regions probed along the wire.

It should be emphasized that we have observed a similar behavior for several bent wires (five were studied in detail). For clarity, in Figure 4 we show a strain investigation of a second wire where we have chosen to probe the part of the wire having the largest curvature (Figure 4b). Raman spectra from selected points along the wire clearly reveal a broadening of the phonon modes as the curvature (and hence strain) is increased. In contrast to the wire in Figure 2, the NW sections at the edge of the selected area shows no strain and accordingly the fwhm of the Raman peaks agree well with the results for the straight wire shown in Figure 1.

We have developed a quantitative description of the strain-induced broadening observed in the bent wires. Following the work of Cerdeira and co-workers[37] and Anastassakis and co-workers,[38] we have used deformation potential theory to calculate strain-induced shifts of the phonon modes assuming uniaxial strain. For simplicity, we have made the assumption that the **k**-vector of the incident light ($\mathbf{k}_{inc}$) is perpendicular to the (110) surface of a slab of InP and that uniaxial strain is applied perpendicular to this direction. The magnitude of the uniaxial strain is determined from the curvature of the wire, being compressive on the

DOI: 10.1021/nl904040y | Nano Lett. 2010, 10, 1280–1286

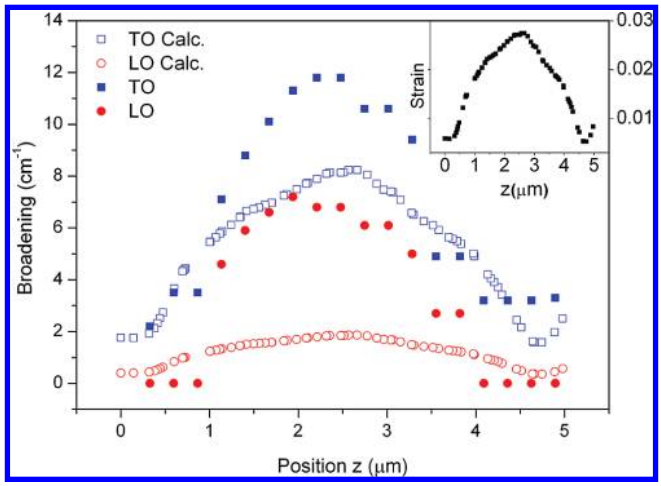

FIGURE 5. Solid markers show the fwhm of the strain-induced broadening component of the Voigt line shape for the TO and LO phonon modes as function of position, (*z*) along the wire shown in Figure 2b, starting at the bottom left (squares, TO and circles, LO). Open markers show the calculated broadening for the two phonon modes (squares, TO and circles, LO). The inset shows the maximum strain at the inside and outside of the curved wire as function of position (*z*), determined from the AFM-measured curvature.

inside and tensional on the outside. For this configuration the strain is expected to mostly affect the TO mode (vibration perpendicular to ($\mathbf{k}_{inc}$)), whereas the LO mode (vibrations parallel to $\mathbf{k}_{inc}$) should be only moderately affected.[37,39] Our model is quite crude since we neglect the detailed shape of the wire, but we expect the results to be accurate to approximately a factor of 2. More detailed modeling would be appropriate were we able to measure the Raman shift at a high enough spatial resolution to compare the inside and the outside of the wire. Since we cannot do this, we have refrained from more elaborate calculations.

Our calculations show that a 1 % strain should induce a broadening of about 1 % for the TO mode and 0.2 % for the LO mode, taking into account the tensile and compressive strain expected for our bent NW system. In Figure 5, we plot the theoretical broadening as function of the position-dependent strain for the wire in Figure 2.

We first discuss the TO phonon modes. The agreement between theory and experiment is reasonable, noting that our calculated values are accurate to about a factor of 2. The comparison shows that Raman spectroscopy indeed is a fast and versatile method to probe structural properties at the nanoscale. The measured and calculated widths of the phonon spectra are in good agreement and both show a slightly asymmetric strain profile along the NW. It should be pointed out that the upturned/flat sections observed for the calculated strain at the very ends of the wire are caused by the smoothing window used when analyzing the wire shape.[31]

To know the detailed atomic structure related to macroscopic changes such as bending is difficult, but there have been several reports on TEM studies involving bending of nanowires.[10,16] These experiments suggest that for polar semiconductor wires, similar to the one used in our study, no plastic deformation is observed, although the wires have been bent as much as 90°. We therefore believe that, as a result of the relatively gentle AFM manipulation technique used here[31] and the moderate strain (<3 %) in our wires, we are working in the elastic regime. This further validates the model we have used for determining the strain along the wire.[10,31]

One expects Raman spectra from regions having dominantly compressive strain to show asymmetric Raman bands with a stronger weight toward higher wave numbers, whereas regions with tensile strain should show peaks weighted on the low wavenumber side. For the bent nanowires, the inner part of the wire is compressively strained whereas the outer part is under tensile stress.[10,13] It was pointed out in ref 10 that it is difficult to determine these strain distributions perpendicular to the axis of nanowires for thin nanowires, since a relatively large volume is sampled in SEM-based cathodoluminescence (about 100 nm). We have also tried to investigate this transverse strain distribution optically by performing linescans perpendicular to the nanowire axis, but at present our method is limited by the rather large probe volume compared to the widths of the nanowires and we do not have sufficient spatial resolution. Further, it is difficult to determine the actual size of the probe volume since it is highly dependent on the polarization of the excitation light, and waveguiding may possibly also occur inside the wires. We have, however, for some positions, observed line shape changes when comparing spectra acquired from an area with the compressive strain to a region with tensile strain. The trend is correct,[10] but higher spatial resolution and better control of size of the probe volume is needed for a reliable interpretation of the data, which for now only show variations comparable to the noise level in our measurements.

By comparing the strain-induced broadening shown in Figure 2a to strain calculations along the wire we estimate the resolution in our setup to be about 300 nm along the wire axis.

For the LO phonon mode we observe that care must be taken when evaluating the strain information obtained from the additional broadening of the Raman spectra. As shown in Figure 5, a discrepancy in the width of the broadening is observed; the calculated broadening is smaller than the experimentally observed value. Since a large N.A. objective was used in our micro-Raman measurement, a considerable amount of light with a $\mathbf{k}$-vector perpendicular to the $\mathbf{k}_{inc}$ illustrated in Figure 1 is present, which was not accounted for in the calculation. This component will broaden the LO mode (but not the TO) more than calculated, restoring agreement between theory and experiment.

It is worthwhile to relate the observed strain-induced broadening to some of the main physical mechanisms for broadening of phonon modes in low dimensional systems; Richter et al. introduced a phenomenological model explain-

DOI: 10.1021/nl904040y | *Nano Lett.* **2010,** *10,* 1280–1286

ing the asymmetry often observed in Raman bands for small semiconductor structures.[40] The model assumes that the confinement ("size effect") is imposed by the surfaces of the nanostructure and was extended to nanowires by Campbell and Fauchet.[41] Many groups have subsequently observed asymmetric broadening of the phonon modes in various NW systems,[22,42] but in all these measurements the NW diameter is very small. Wires with diameters larger than 20 nm show almost no asymmetrical downshift of the phonon modes,[22] and thus we exclude such effects for the wires used in our experiments.

Surface optical (SO) phonon modes are confined to a region near the surface of a material and have frequencies that lie between the TO and LO modes of the bulk material. Their exact position is dependent on the wave vector along the surface as well as the dielectric functions of the material and its surroundings.[43,44] Raman spectra from semiconductor nanowires have been reported to show strong SO modes.[23] Intriguingly, one would not expect the SO modes to be optically detectable for an ideal NW due to momentum conservation. Experimental results suggest that this constraint can be overcome by a "grating" effect arising from small periodic spatial variations along the wires.[18,19,22]

To assess the effects of SO phonons in our samples, we measured Raman spectra on individual NWs before and after embedding the wires in PMMA (thereby drastically changing the dielectric function of the surrounding media). The high dielectric constant of the embedding material is expected to influence any SO modes that are present. However, our measurements show no spectral differences upon embedding the wires. Analytical calculations following ref 43 indicate that the downshift of an SO mode should be clearly detectable in our setup for wires having diameters of 40−70 nm. We therefore conclude that no SO modes are present in our Raman spectra, in contrast with recent papers.

It is a desirable but delicate task to reveal details of the material properties of nanometer-sized structures with high spatial resolution, but in a noninvasive way. We have shown that Raman spectroscopy is a suitable technique that probes the local strain in individual semiconductor nanowires. Deformation potential theory, using strain values derived from careful analysis of the wire shape, reproduces the observed broadening of the Raman spectra in a quantitative manner. However, detailed knowledge of the sample geometry, surface crystal planes, and so forth are needed to determine the optical field distribution in nanostructures properly. In future experiments, tip-enhanced Raman spectroscopy[45−47] could provide improved spatial resolution, paving the way for new interesting investigations of semiconductor nanowire systems. Of immediate interest would be to investigate how different dopants, doping concentrations, or even different crystal polytypes affect the material properties on a local scale.

Acknowledgment. We acknowledge Mariusz Graczyk and David Adolph for assistance in sample processing and Professor Håkan Pettersson and Nicklas Anttu for stimulating discussions. This work was performed within the Nanometer Structure Consortium at Lund University and was supported by the Swedish Research Council (VR), the Swedish Foundation for Strategic Research (SSF), the Crafoord Foundation, and the Knut and Alice Wallenberg Foundation.

Supporting Information Available. This material is available free of charge via the Internet at http://pubs.acs.org.

REFERENCES AND NOTES

(1) Gudiksen, M. S.; Lauhon, L. J.; Wang, J.; Smith, D. C.; Lieber, C. M. *Nature* **2002**, *415* (6872), 617–620.
(2) Pauzauskie, P. J.; Yang, P. *Mater. Today* **2006**, *9* (10), 36–45.
(3) Thelander, C.; Agarwal, P.; Brongersma, S.; Eymery, J.; Feiner, L. F.; Forchel, A.; Scheffler, M.; Riess, W.; Ohlsson, B. J.; Gosele, U.; Samuelson, L. *Mater. Today* **2006**, *9* (10), 28–35.
(4) Algra, R. V., M. A.; Borgström, M. T.; Feiner, L. F.; Immink, G.; van Enckevort, W. J. P.; Vlieg, E.; Bakkers, E. P. A. M. *Nature* **2008**, *456*, 369–372.
(5) Caroff, P. D., K. A.; Johansson, J.; Messing, M. E.; Deppert, K.; Samuelson, L. *Nat. Nanotechnol.* **2009**, *4*, 50–55.
(6) Pistol, M.-E.; Gerling, M.; Hessman, D.; Samuelson, L. *Phys. Rev. B* **1992**, *45* (7), 3628–3635.
(7) Pistol, M.-E.; Pryor, C. P. *Phys. Rev. B* **2009**, *80*, No. 035316.
(8) Wang, X. D.; Zhou, J.; Song, J. H.; Liu, J.; Xu, N. S.; Wang, Z. L. *Nano Lett.* **2006**, *6* (12), 2768–2772.
(9) Lin, X.; He, X. B.; Yang, T. Z.; Guo, W.; Shi, D. X.; Gao, H. J.; Ma, D. D. D.; Lee, S. T.; Liu, F.; Xie, X. C. *Appl. Phys. Lett.* **2006**, *89* (4), No. 043103.
(10) Han, X.; Kou, L.; Lang, X.; Xia, J.; Wang, N.; Qin, R.; Lu, J.; Liao, Z.; Zhang, X.; Shan, X.; Song, X.; Gao, J.; Guo, W.; Yu, D. *Adv. Mater.* **2009**, *21*, 4937.
(11) Bjork, M. T.; Ohlsson, B. J.; Sass, T.; Persson, A. I.; Thelander, C.; Magnusson, M. H.; Deppert, K.; Wallenberg, L. R.; Samuelson, L. *Nano Lett.* **2002**, *2* (2), 87–89.
(12) Larsson, M. W.; Wagner, J. B.; Wallin, M.; Hakansson, P.; Froberg, L. E.; Samuelson, L.; Wallenberg, L. R. *Nanotechnology* **2007**, *18* (1), 015504.
(13) Zheng, K.; Han, X. D.; Wang, L. H.; Zhang, Y. F.; Yue, Y. H.; Qin, Y.; Zhang, X. N.; Zhang, Z. *Nano Lett.* **2009**, *9* (6), 2471–2476.
(14) Lopez, F. J.; Hemesath, E. R.; Lauhon, L. J. *Nano Lett.* **2009**, *9* (7), 2774–2779.
(15) Bell, D. C.; Wu, Y.; Barrelet, C. J.; Gradecak, S.; Xiang, J.; Timko, B. P.; Lieber, C. M. *Microsc. Res. Tech.* **2004**, *64* (5−6), 373–389.
(16) Larsson, M. W.; Wallenberg, R. W.; Persson, A. I.; Samuelson, L. *Microsc. Microanal.* **2004**, *10*, 41–46.
(17) Weber, W. H.; Merlin, R. *Raman Scattering in Material Science*; Springer: Berlin, 2000; Vol. 42.
(18) Gupta, R.; Xiong, Q.; Mahan, G. D.; Eklund, P. C. *Nano Lett.* **2003**, *3* (12), 1745–1750.
(19) Begum, N.; Piccin, M.; Jabeen, F.; Bais, G.; Rubini, S.; Martelli, F.; Bhatti, A. S. *J. Appl. Phys.* **2008**, *104* (10), 104311.
(20) Spirkoska, D.; Abstreiter, G.; I Morral, A. F. *Nanotechnology* **2008**, *19* (43), 435704.
(21) Pauzauskie, P. J.; Talaga, D.; Seo, K.; Yang, P. D.; Lagugne-Labarthet, F. *J. Am. Chem. Soc.* **2005**, *127* (49), 17146–17147.
(22) Adu, K. W.; Xiong, Q.; Gutierrez, H. R.; Chen, G.; Eklund, P. C. *Appl. Phys. A* **2006**, *85* (3), 287–297.
(23) Xiong, Q. H.; Wang, J. G.; Reese, O.; Voon, L.; Eklund, P. C. *Nano Lett.* **2004**, *4* (10), 1991–1996.
(24) Xing, Y. J.; Xi, Z. H.; Xue, Z. Q.; Zhang, X. D.; Song, J. H.; Wang, R. M.; Xu, J.; Song, Y.; Zhang, S. L.; Yu, D. P. *Appl. Phys. Lett.* **2003**, *83* (9), 1689–1691.
(25) Mahan, G. D.; Gupta, R.; Xiong, Q.; Adu, C. K.; Eklund, P. C. *Phys. Rev. B* **2003**, *68* (7), No. 073402.
(26) Mahan, G. D. *Phys. Rev. B* **2006**, *74* (3), No. 033407.

DOI: 10.1021/nl904040y | *Nano Lett.* **2010,** *10,* 1280–1286

(27) Adu, K. W.; Gutierrez, H. R.; Kim, U. J.; Sumanasekera, G. U.; Eklund, P. C. *Nano Lett.* **2005**, *5* (3), 409–414.
(28) Piscanec, S.; Cantoro, M.; Ferrari, A. C.; Zapien, J. A.; Lifshitz, Y.; Lee, S. T.; Hofmann, S.; Robertson, J. *Phys. Rev. B* **2003**, *68* (24), 241312.
(29) Chen, G.; Wu, J.; Lu, Q. J.; Gutierrez, H. R. H.; Xiong, Q.; Pellen, M. E.; Petko, J. S.; Werner, D. H.; Eklund, P. C. *Nano Lett.* **2008**, *8* (5), 1341–1346.
(30) Bordag, M.; Ribayrol, A.; Conache, G.; Froberg, L. E.; Gray, S.; Samuelson, L.; Montelius, L.; Pettersson, H. *Small* **2007**, *3* (8), 1398–1401.
(31) Conache, G.; Gray, S. M.; Ribayrol, A.; Froberg, L. E.; Samuelson, L.; Pettersson, H.; Montelius, L. *Small* **2009**, *5* (2), 203–207.
(32) Borgstrom, M. T.; Norberg, E.; Wickert, P.; Nilsson, H. A.; Tragardh, J.; Dick, K. A.; Statkute, G.; Ramvall, P.; Deppert, K.; Samuelson, L. *Nanotechnology* **2008**, *19* (44), 445602.
(33) Mooradia, A.; Wright, G. B. *Solid State Commun.* **1966**, *4* (9), 431–434.
(34) Wang, J. F.; Gudiksen, M. S.; Duan, X. F.; Cui, Y.; Lieber, C. M. *Science* **2001**, *293* (5534), 1455–1457.
(35) Xiong, Q.; Chen, G.; Gutierrez, H. R.; Eklund, P. C. *Appl. Phys. A* **2006**, *85* (3), 299–305.
(36) Sirbuly, D. J.; Law, M.; Yan, H. Q.; Yang, P. D. *J. Phys. Chem. B* **2005**, *109* (32), 15190–15213.
(37) Cerdeira, F.; Buchenau, C. J.; Cardona, M.; Pollak, F. H. *Phys. Rev. B* **1972**, *5* (2), 580–593.
(38) Anastassakis, E.; Raptis, Y. S.; Hunermann, M.; Richter, W.; Cardona, M. *Phys. Rev. B* **1988**, *38* (11), 7702–7709.
(39) Anastassakis, E. *J. Appl. Phys.* **1997**, *82* (4), 1582–1591.
(40) Richter, H.; Wang, Z. P.; Ley, L. *Solid State Commun.* **1981**, *39* (5), 625–629.
(41) Campbell, I. H.; Fauchet, P. M. *Solid State Commun.* **1986**, *58* (10), 739–741.
(42) Wang, R. P.; Zhou, G. W.; Liu, Y. L.; Pan, S. H.; Zhang, H. Z.; Yu, D. P.; Zhang, Z. *Phys. Rev. B* **2000**, *61* (24), 16827–16832.
(43) Watt, M.; Torres, C. M. S.; Arnot, H. E. G.; Beaumont, S. P. *Semicond. Sci. Technol.* **1990**, *5* (4), 285–290.
(44) Ruppin, R.; Englman, R. *Rep. Prog. Phys.* **1970**, *33* (2), 149–196.
(45) Anderson, N.; Hartschuh, A.; Cronin, S.; Novotny, L. *J. Am. Chem. Soc.* **2005**, *127* (8), 2533–2537.
(46) Bailo, E.; Deckert, V. *Angew. Chem., Int. Ed.* **2008**, *47* (9), 1658–1661.
(47) Hartschuh, A.; Sanchez, E. J.; Xie, X. S.; Novotny, L. *Phys. Rev. Lett.* **2003**, *90* (9), No. 095503.

DOI: 10.1021/nl904040y | *Nano Lett.* **2010,** *10,* 1280–-1286